Proceedings of the 4th International Conference on Fluid Flow and Thermal Science (ICFFTS'23)
Lisbon, Portugal- December 07 - 09, 2023
Paper No. 164
DOI: 10.11159/icffts23.164

Variable PCM Density-based Numerical Model for Packed Bed Latent Heat Thermal Energy Storage

Akshay Kumar[1], Sandip K. Saha[1]
[1]Indian Institute of Technology Bombay
Department of Mechanical Engineering, IIT Bombay, Mumbai- 400076, INDIA.
174109001@iitb.ac.in; sandip.saha@iitb.ac.in

Abstract **-** This work focuses on developing a numerical model for packed bed latent heat thermal energy storage with cylindrical-shaped encapsulation of phase change material (PCM). A local thermal non-equilibrium model with a porous media approach is developed. The effect of shrinkage and expansion of PCM during melting and solidification are considered. The PCM density is modelled as the function of melt fraction, liquid and solid density of PCM. The latent heat part of PCM is modelled using the enthalpy-porosity approach. The flow of heat transfer fluid (HTF) over the cylindrical particles is considered a cross-flow arrangement. In this numerical modelling, three equations for HTF (mass, momentum and energy) and one energy equation for PCM and storage tank wall are solved. The main purpose was to develop a computationally efficient model that can capture and incorporate the shrinkage and expansion effect of PCM while melting and solidification.

Keywords**:** Cylindrical encapsulation, phase change material, shrinkage and expansion, thermal energy storage, packed bed

1. Introduction

One of the significant causes of air pollution is the production of energy by burning fossil fuels. To reduce air pollution, the use of renewable energy sources is imminent, and the investment in clean energy production has been increasing for a few years. The investment in clean energy production will surpass 2 trillion USD by 2030 [1]. Among the renewable energy sources, solar energy has the potential to overcome the energy need. It can be used efficiently for power generation as well as domestic applications. However, there is a need for a thermal energy storage system to make the solar energy supply continuous. Latent heat thermal energy storage (LHTES) is an optimum choice for storage because of its higher storage capacity with lesser temperature variation [2-3]. In LHTES, PCM goes through several melting and solidification cycles to store and retrieve thermal energy. Several researchers applied the PCM-based LHTES for different applications such as thermal solar power generation [4-5], and thermal cooling of electronics equipment [6]. Most of the PCMs have lower thermal conductivity, which results in a lower heat transfer rate. Various researchers reported the heat transfer improvement method from PCM to HTF, such as encapsulation of PCM [7-9], and the addition of metal matrix and fins [10]. The encapsulation of PCM is one of the heat transfer enhancement methods. The research work on the encapsulation of PCM for LHTES has been carried out numerically as well as experimentally [11-12]. Most of the work is carried out for the spherical shape of encapsulation and has not considered the shrinkage and expansion effect of PCM during melting and solidification in the LHTES system.

In the present work, a numerical model is developed for packed bed latent heat thermal energy storage (PBTES) with cylindrical-shaped encapsulation of PCM. The shrinkage and expansion effect of PCM is considered by incorporating the equivalent density of the PCM into the energy equation of PCM. The equivalent density of the PCM is taken as the function of the melt fraction of the PCM, liquid and solid density of the PCM.

2. Physical domain and Numerical modelling

The physical domain consists of a cylindrical tank with cylindrical PCM capsules. The HTF enters from the top of the tank and flows through the pores between PCM capsules. The flow of HTF is modelled using the porous medium approach. The material of encapsulation is taken as stainless steel. The flow of HTF over the cylindrical capsules is assumed to be cross-flow.

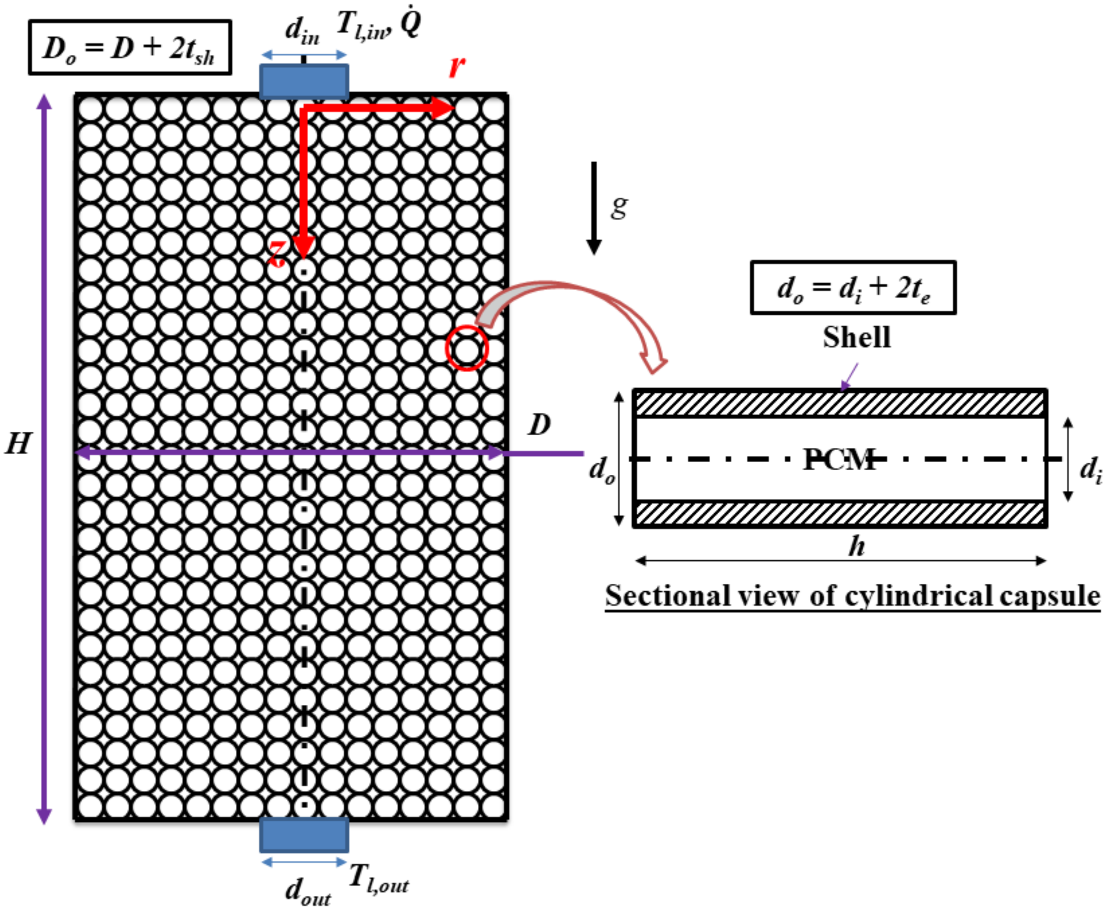

Fig. 1: Schematic of thermal energy storage with cylindrical PCM capsule

2.1. Conservation of mass for HTF

$$\frac{\partial(\phi\rho_l)}{\partial t} + \nabla.(\rho_l\vec{u}) = 0 \tag{1}$$

where ϕ represents the porosity of the packed bed. ρ_l & $\vec{u}$ represents the density and velocity vector of heat transfer fluid (HTF).

2.2. Conservation of momentum for HTF

$$\frac{1}{\phi}\frac{\partial(\rho_l\vec{u})}{\partial t} + \frac{\vec{u}}{\phi}\nabla.\left(\rho_l\frac{\vec{u}}{\phi}\right) = -\nabla P + \frac{\mu}{\phi}\nabla^2\vec{u} + \rho_l g + S_1 \tag{2}$$

In the conservation of momentum for HTF, the term S_1 represents the momentum sink term due to the resistance of flow through the porous media. The modelling of the momentum sink term is adopted from the Forchheimer expression [13]. The expression consists of inertial losses as well as viscous losses such as,

$$S_1 = -\left(\frac{\mu\vec{u}}{\varepsilon} + C_2\frac{\rho_l|\vec{u}|\vec{u}}{2}\right) \tag{3}$$

The permeability (ε) and inertial coefficients (C_2) are found using the Ergun expression [14] as,

$$\varepsilon = \frac{d_{eq}^2 \phi^3}{150(1-\phi)^2} \tag{4}$$

$$C_2 = \frac{1.75(1-\phi)}{d_{eq}\phi^3} \tag{5}$$

where d_{eq} represents the equivalent diameter of cylindrical particles. The Ergun equation is developed for spherical shapes of particles. To apply the Ergun equation for non-spherical particles, the equivalent diameter is estimated using the porous media flows for non-spherical particles [15].

2.3. Conservation of energy for HTF

$$\frac{\partial(\phi\rho_l c_{p,l} T_l)}{\partial t} + \nabla.\left(\rho_l c_{p,l} T_l \vec{u}_l\right) = \nabla.(k_l \nabla T_l) + h_{oi,vol}(T_s - T_{al}) + h_{w,vol}(T_w - T_l) \tag{5}$$

where $h_{oi,vol}$ is the volumetric heat transfer coefficient between the PCM capsule and HTF. $h_{w,vol}$ represents the heat transfer coefficient between the storage tank wall and HTF. The convection coefficient is found using the correlation of cross-flow over the cylinder [16]. T_l and $c_{p,l}$ represent the temperature and specific heat of HTF. T_w represent the storage tank wall temperature.

2.4. Conservation of energy for PCM

$$\frac{d\left[(1-\phi)\rho_{eq} c_{P,eq} T_s\right]}{dt} = \nabla.\left(k_{eq} \nabla T_s\right) + h_{oi,vol}(T_l - T_s) + S_2 \tag{6}$$

where $S_2 = -\frac{d[(1-\phi)\rho_{sol}\Delta E]}{dt}$ is an unsteady source term to add the latent heat content of PCM during melting and solidification. The phase change of PCM is modelled using the enthalpy porosity technique [17]. For a constant-temperature phase change, the nodal latent heat content (ΔE) for the **P^th^** control volume after the n^{th} iteration is updated as,

$$[\Delta E_p]_{n+1} = [\Delta E_p]_n + \frac{a_p}{a_p^0} c_{p,sol} \lambda\left([T_{s,p}]_n - T_{sol}\right) \tag{7}$$

where T_s and $c_{P,eq}$ represent the temperature and specific heat of PCM. k_{eq} defines the thermal conductivity of PCM. To avoid the latent heat content from non-realistic values, the following limits are set.

$$[\Delta E_p]_n = 0 \; if \; [\Delta E_p]_{n+1} < 0 \tag{8}$$

$$[\Delta E_p]_n = L \; if \; [\Delta E_p]_{n+1} > L \tag{9}$$

In this model, the PCM properties are taken separately for liquid and solid phases. The ρ_{eq} represents the equivalent density of the PCM and is defined as,

$$\rho_{eq} = f\rho_{liq} + (1-f)\rho_{sol} \tag{8}$$

where f represents the melt fraction of the PCM. ρ_{liq} and ρ_{sol} represents the liquid and solid density of PCM.

2.5. Conservation of energy for storage tank wall

$$\rho_w c_{p,w} \forall \frac{\partial T_w}{\partial t} = \nabla \cdot (k_w \nabla T_w) + h_{w,vol}(T_a - T_w) - h_{conv,amb}\left(T_w - T_{amb}\right) \tag{10}$$

In the above equation, $h_{conv,amb}$ is the volumetric convection coefficient between the ambient and outer surface of the storage tank. $\forall$ is defined as storage tank wall volume per internal volume of the energy storage tank.

A new solver is developed in OpenFOAM V6 environment. For airflow through the porous medium, the SIMPLE algorithm is used to model the pressure-velocity coupling. Euler's first-order implicit scheme is applied to model the term.

3. Validation of Numerical model for cylindrical capsule

The currently developed numerical model is compared and validated with the in-house experimental results of cylindrical-shaped encapsulation. In the validation study considering cylindrical capsules, the TES is a vertical cylinder with length (H) = 300 mm and diameter (D) = 215 mm. A eutectic mixture of $NaNO_3$ and KNO_3 in the weight ratio 60:40 named solar salt is chosen as a PCM and air is used as HTF. As shown in Figure 2, the experimental setup consists of a 2 HP air blower to supply the air throughout the flow circuit, an electric air heater, a Coriolis mass flowmeter to measure the mass flow rate of air and a counter flow heat exchanger to cool the exhaust air. The numerical model is validated for charging as well as discharging.

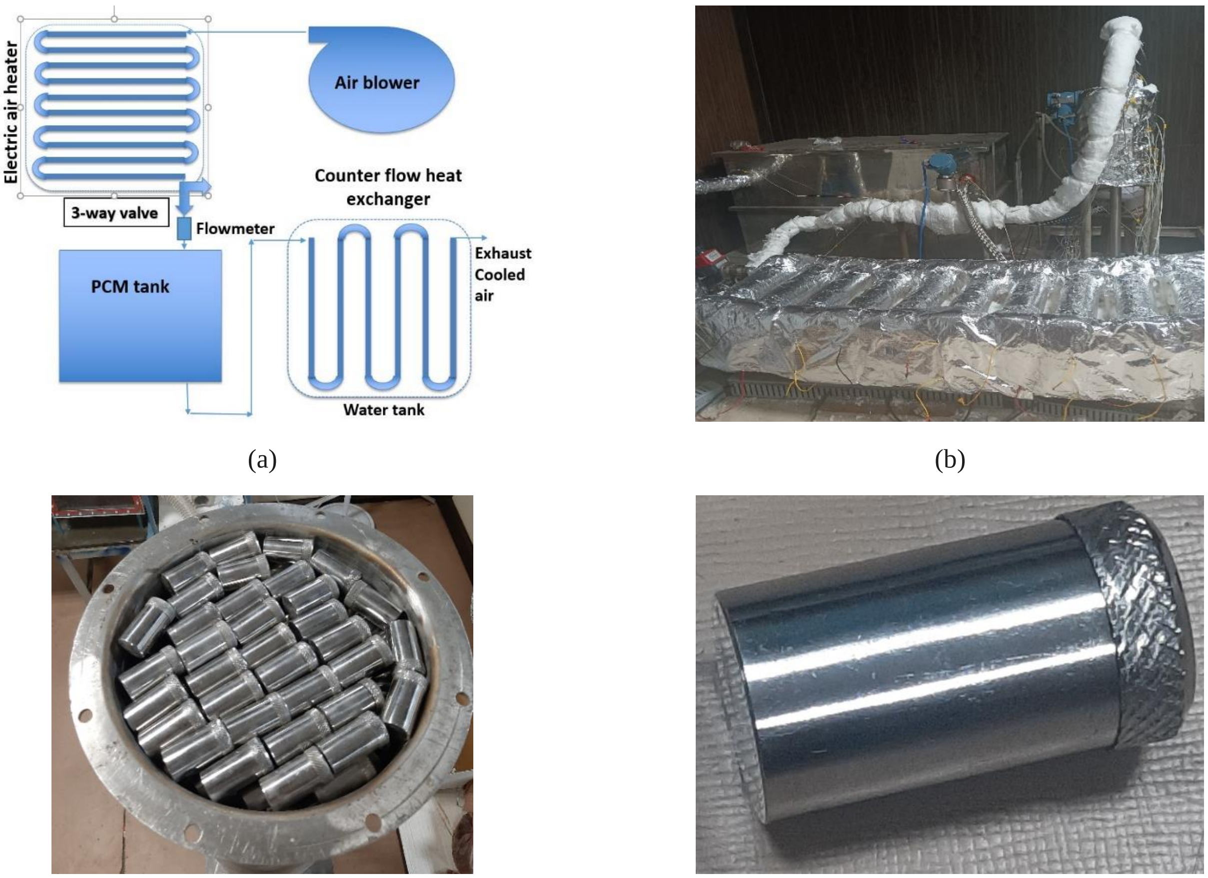

Fig. 2: (a) Schematic of flow through the experimental setup (b) in-house developed setup (c) Front-view of packed bed (d) Cylindrical capsule

The mathematical formulation of boundary condition is as follows,

<u>Initial conditions</u>

(a) $T_{ini} = 28\ °\text{C}$ at t = 0 s (Charging) and $T_{ini} = 240\ °\text{C}$ at t = 0 s (Discharging)

<u>Boundary conditions</u>

(b) Inlet: for Charging: T_{air} is varied with time. For charging and discharging, $T_{air,d} = 32$ °C, $\dot{m} = 4.3\ g/s$

(c) Outlet: $\frac{dP}{dz} = 0$, $\frac{dT_{air}}{dz} = 0$

(d) Surface (Wall): $\frac{dT_{air}}{dr} = 0, \frac{dT_{PCM}}{dr} = 0$, $u = v = 0$

Axis: $\frac{dT_{air}}{dr} = 0$

Table 1 shows all the parameters considered in this numerical validation. The properties of air, solar salt and SS316 are taken as per Table 2. There is a significant difference between the solid and liquid density of solar salt. Therefore, it is crucial to incorporate the shrinkage and expansion effects. The air properties also listed in Table 2.

Table 1: Various parameters considered in the validation study

Volume flow rate	4.3 g/s
PCM initial temperature	32 °C
HTF	Air
PCM	Solar salt
Inside diameter of PCM cylindrical capsule	18 mm
Outside diameter of PCM capsule	21.3 mm
Total number of capsules	402
Porosity	0.47
Length of storage tank	300 mm
Diameter of storage tank	215 mm

Table 2: Thermophysical properties of Air and PCM

Properties	**Air**	**Solar salt**	**SS316**
ρ_{sol} (kg/m^3)	1.2	2193	8030
ρ_{liq} *(kg/m^3)*	-	1794	-
c_p (J/kg.K)	1005	1380	502.48
k (W/m.K)	0.028	0.65	16
μ (kg/m.s)	1.8×10^{-5}	0.0021	-
T_m (°C)		220	-
L (kJ/kg)		132	-

In the validation study, a stand-alone charging and discharging process is conducted. A comparative study is carried out to compare the experimental temperature of the air at the outlet of the storage system and PCM temperature with the present shrinkage numerical model, which is shown in Figure 3(a) and Figure 3(b). In this experiment, the air temperature at the inlet of the storage system varies with the time during the charging process, whereas it is taken as 32 °C during the discharging process. Figure 3(a) and Figure 3(b) show that the air outlet temperature, as well as PCM temperature with the shrinkage numerical model, are closer to the experimental results. For the charging and discharging process, the mean absolute deviation between experimental and numerical results for the air outlet temperature is found to be 3.75%. It can be noted that in this numerical model, the advection of the melt PCM is not considered. For the charging process, the PCM temperature at the axial distance of 90 mm from the inlet of the tank is also validated, as shown in Figure 3(a). For PCM temperature validation, a single capsule model is simulated by applying the temporal variation of experimental temperature at the surface of a single microcapsule. The model is also validated for the PCM temperature during discharging at the axial location of 270 mm from the inlet of the tank, as shown in Figure 3(b). The present numerical model agrees well with the experimental results of the outlet air and the single microcapsule PCM temperatures. This numerical model is more computationally efficient than simulating each capsule in a packed bed thermal energy storage system.

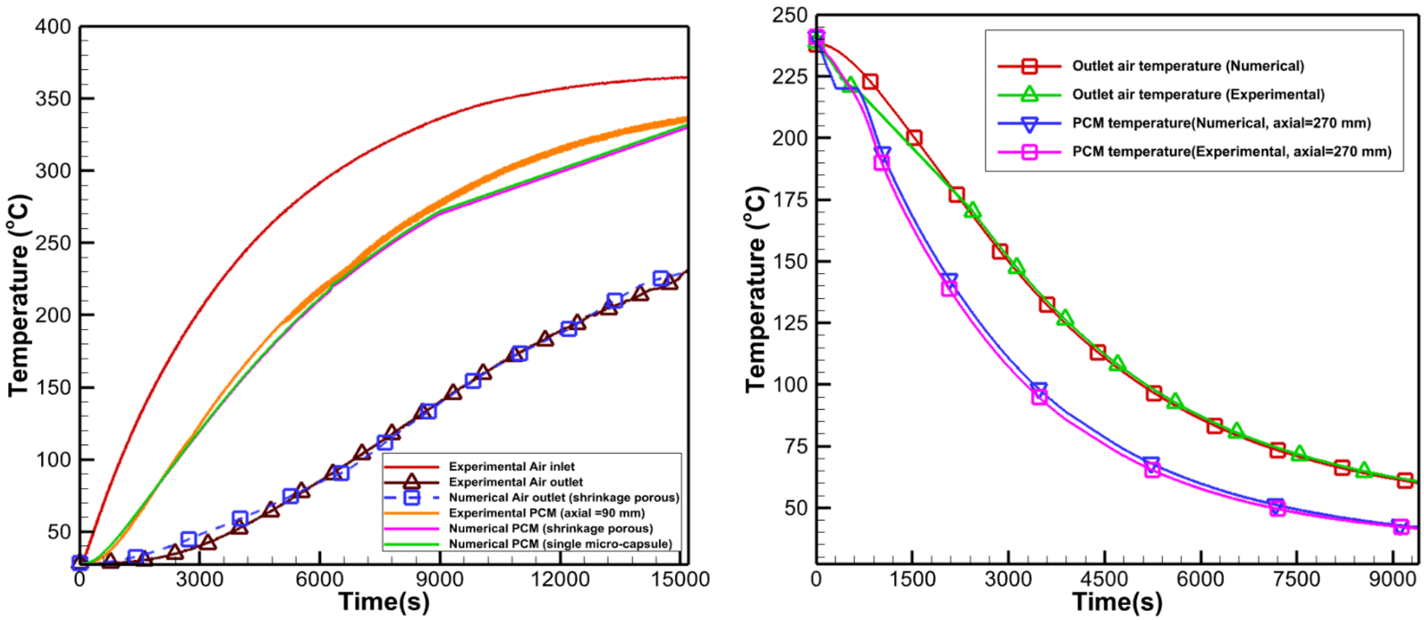

(a) (b)

Fig. 3: Validation of the numerical model for air outlet temperature and PCM temperature for (a) charging process and (b) discharging process

4. Conclusion

In the present work, a numerical model of packed bed thermal energy storage with cylindrical-shaped encapsulation of PCM is developed. The effect of shrinkage and expansion while phase transformation is incorporated into the energy equation of PCM. The density of the PCM is taken as the function of the melt fraction of the PCM. The numerical model is validated with an in-house developed experimental setup. The solar salt with a melting point of 220 °C is considered as PCM and air as the HTF. It is found that this shrinkage porous model fits with the experimental results without solving the momentum equation for PCM. It gives the same PCM temperature as compared to prediction with a single micro-capsule of PCM at the same location in PBTES. The shrinkage porous model is more computationally efficient as compared to the single micro-capsule model for a packed bed system. The model fits well with a mean absolute deviation of 3.75%.

Acknowledgement

The authors acknowledge the financial support from the Department of Science and Technology, India (grant number: DST/TMD/MES/2K17/25(C)).

References

[1] World energy outlook 2022, International Energy Agency (IEA)

[2] A. Sharma, V. Tyagi, C.R. Chen, D. Buddhi, "Review on thermal energy storage with phase change materials and applications", *Renew. Sust. Energy Rev.*, 2009, vol. 13, pp 318–345.

[3] Z. Yang, S.V. Garimella, "Molten-salt thermal energy storage in thermoclines under different environmental boundary conditions", *Applied Energy,* 2010, vol. 87, pp 3322-2239.

[4] H. Michels, R. Pitz-Paal, "Cascaded latent heat storage for parabolic trough solar power plants", *Sol. Energy*, 2007, vol. 81, pp 829–837.
[5] A. Gil, M. Medrano, I Martorell, A. Lázaro, P. Dolado, B. Zalba, L.F. Cabeza, "State of the art on high-temperature thermal energy storage for power generation. Part 1-Concepts, materials and modellization." *Renew. Sustain. Energy Rev*. 2010, vol. 14, pp 31–55.
[6] S.K. Saha, P. Dutta, "Performance Analysis of heat sinks with phase-change materials subjected to transient and cyclic heating", *Heat Transfer Engineering*, 2015, vol. 36, pp 1349-1359
[7] A. Kumar, S. K. Saha, "Performance analysis of a packed bed latent heat thermal energy storage with cylindrical-shaped encapsulation", *Int. J. Energy Res.*, 2021, vol. 45, pp 13130- 13148.
[8] A. Kumar, S. K. Saha, "Thermal and structural characterizations of packed bed thermal energy storage with cylindrical micro-encapsulated phase change materials", *Journal of Energy Storage*, 2022, vol. 48, pp 103948
[9] R. Senthil, P. Sundaram, M. Kumar," Experimental investigation on packed bed thermal energy storage using paraffin wax for concentrated solar collector", *Materials Today: Proceedings*, 2018, vol. 5, pp 8916-8922.
[10] A. Kumar, S.K. Saha, "Latent heat thermal storage with variable porosity metal matrix: A numerical study," *Renewable Energy*, 2018, vol. 125, pp 962-973.
[11] K. Bhagat, S.K. Saha, "Numerical analysis of latent heat thermal energy storage using encapsulated phase change material for solar thermal power plant", *Renewable Energy*, 2016, vol.95, pp 323-336
[12] A. Raul, M. Jain, S. Gaikwad, S. K. Saha, "Modelling and experimental study of latent heat thermal energy storage with encapsulated PCMs for solar thermal applications", *Applied Thermal Engineering*, 2018, vol. 143, pp 415-428.
[13] P. Forchheimer, Wasserbewegung durch Boden, Z. Ver. Deutsch, Ing., 1901, vol. 45, pp 1782-1788.
[14] S. Ergun, "Fluid flow through packed columns*", Chem. Eng.Prog*. ,1952, vol. 48, pp 89-94.
[15] L. Li, W. Ma, "Experimental study on the effective particle diameter of a packed bed with non-spherical particles", *Transp. Porous. Med.*, 2011, vol. 89, pp 35-48.
[16] S.W. Churchill, M. Bernstein, "A correlating equation for forced convection from gases and liquids to a circular cylinder in cross-flow", *ASME J. Heat Transfer*, 1977, vol. 99, pp 300-306.
[17] A.D. Brent, V.R. Voller, K.J. Reid, "Enthalpy-porosity technique for modelling convection-diffusion phase change: application to the melting of a pure metal", *Numerical Heat Transfer*,1988, vol. 13, pp 297-318.